

Single Crystal Growth of Aluminum Nitride

Hiroyuki Kamata¹, Yuu Ishii², Toshiaki Mabuchi³, Kunihiro Naoe¹,
Shoji Ajimura⁴, Kazuo Sanada⁵

Single crystalline aluminum nitride (AlN) is a promising material used as a substrate for the purpose of improving the performance of AlN-based III-nitride semiconductors that are expected to be used in high power, RF electronic devices and deep UV LEDs/LDs. Sublimation method with open-system crucibles was chosen for single crystal growth of AlN because open-system growth is helpful in understanding the effects of parameters on crystal growth and has the extended degree of freedom in the selection of growth conditions. As a result of the crystal growth, millimeter-sized AlN single crystals with a dislocation density less than 10^7 cm^{-2} were grown on SiC substrates.

1. Introduction

AlN has the broadest band gap energy (6.2 eV) in semiconductors and superior properties of electric breakdown field ($11.7 \text{ MV} \cdot \text{cm}^{-1}$), electron mobility ($1100 \text{ cm}^2 \cdot \text{V}^{-1} \cdot \text{s}^{-1}$) and thermal conductivity ($3.4 \text{ W} \cdot \text{cm}^{-1} \cdot \text{K}^{-1}$). Physical properties of important semiconductors are shown in Table 1¹⁾³⁾. Nowadays, SiC and GaN are attracting attention as substitutes for Si semiconductors and are expected to be used as high power and energy-saving power electronics and RF devices. The use of AlN has led to the possibility of an electronic semiconductor device with higher performance than those because it has superior properties of electrical breakdown and electron transport.

AlN is a direct semiconductor, suitable for light emitting devices. Recently, AlN light-emitting diodes (LED) with wavelength of deep-ultraviolet (DUV) region were demonstrated⁴⁾. So, AlN-based DUV LEDs and laser diodes will be put to practical use in the near future.

It is necessary to grow highly textured epitaxial layers to take advantage of the excellent potential of AlN-based nitride semiconductors. Single crystalline AlN substrates are desirable because of their good lattice matching with AlN-based nitrides. However, there are few AlN substrates that have been produced as a semiconductor grade with satisfactory caliber and crystal-line quality to date.

AlN sublimes by heating in an atmospheric pressure since it has a high dissociation pressure of nitrogen. Then, we selected a seeded sublimation method

Table 1. Physical properties of Si and representative wide band gap semiconductors.

Item	AlN	Si	GaAs	4H-SiC	GaN	Diamond
Band gap energy/eV	6.28 ²⁾	1.12	1.43	3.26	3.39	5.47
Electron mobility/ $\text{cm}^2 \cdot \text{V}^{-1} \cdot \text{s}^{-1}$	1100	1350	8500	720 ^{a)} / 650 ^{c)}	900	1900
Electric breakdown field/ $10^6 \text{ V} \cdot \text{cm}^{-1}$	11.7	0.3	4.0	2.0	3.3	5.6
Thermal conductivity/ $\text{W} \cdot \text{cm}^{-1} \cdot \text{K}^{-1}$	3.4 ³⁾	1.5	0.5	4.5	1.3	20
Band type	D	I	D	I	D	I

a: a-pole direction, c: c-pole direction
D: Direct transition type, I: Indirect transition type

for AlN growth and have investigated the technique. In this method the sublimed gas from the source is transported to the colder seed crystal by diffusion and condensed to form crystals in quasi-closed space. In case of AlN, sublimation and crystal growth is shown by the following equations respectively.



The formation of single crystalline AlN involves nitrogen gas as shown in eq.(2). Thus, we chose using an open-system crucible to introduce nitrogen into crucible. For the closed-system sublimation method, AlN is crystallized from the gas composed of stoichiometric Al/nitrogen ratio sublimed from the source and cannot be changed. On the other hand, controlling the sublimation rate of the source and nitrogen flow rate can change the ratio in the open system. In addition,

1 : Metallic Material Department of Materials Technology Laboratory
2 : Circuit Technology R&D Department
3 : Engineering Department of Thermal Technology Division
4 : Connector Division
5 : R&D Planning Department

the open-system growth helps in understanding the effects of parameters on crystal growth and has the extended degree of freedom in the selection of growth conditions. Once a single crystal growth condition is established, it is possible to designedly control the parameters with a good reproducibility. In this paper, the results of single crystal growth of AlN on SiC substrates are presented.

2. Experimental procedure

Single crystal growth of AlN was conducted using an RF-induction furnace with a graphite crucible. Si-face, on- and off-axis (0001) 6H-SiC substrates with thickness of 380 μm were employed as seeds. The schematic illustration of the open-system crucible used for AlN growth is shown in Fig. 1. AlN powder in a graphite container was set at the bottom of the crucible. SiC seed was fixed on the crucible lid. The crucible was heated and the sublimation gas from the source was mixed with nitrogen through the inlet using a mass flow controller. The gas mixture was transported to the colder SiC seed and crystallized as AlN. The exhaust gas was flown out of the crucible through the outlet.

Temperatures of growth and sublimation were controlled by monitoring the back of the susceptor and the bottom of the crucible by dual-color infrared pyrometers, respectively. Crystal growth was performed at 2273 K for 1.5~30 h. An ambient pressure was kept constant by using a pressure controller with a butterfly valve.

The crystallographic orientation of grown crystals was identified by X-ray diffraction (XRD) measurement by θ -2 θ scan and pole figure using the $\text{CuK}\alpha$ line. Their crystalline quality was evaluated by X-ray rocking curves (XRCs) of AlN (0002). Surface and cross-section of the samples were observed by optical microscopy (OM), scanning electron microscopy (SEM) and transmission electron microscopy (TEM).

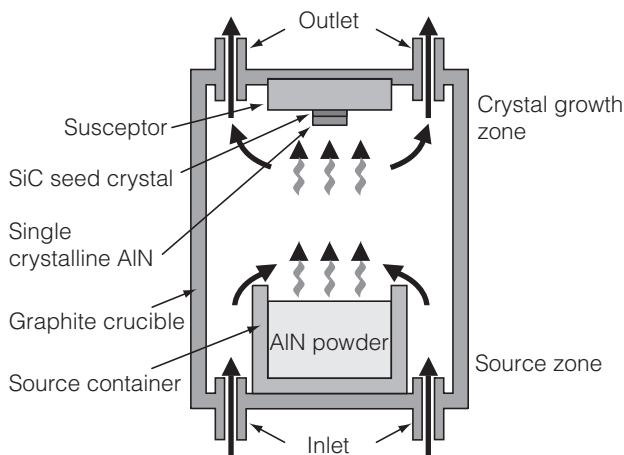


Fig. 1. Schematic illustration of a growth crucible

3. Results and discussion

3.1 AlN crystal growth on on-axis SiC (0001)

The experiments were performed for a short time of 1.5 h to search growth conditions of single crystalline AlN. OM and SEM images of SiC seeds after AlN growth are shown in Fig. 2. At first, AlN grown on SiC was poly-crystalline granular precipitates like the sample A shown in Fig. 2 (a) and (b). As a result of investigation of growth conditions, we obtained a transparent-colorless layer with smooth surface like the sample B shown in Fig. 2 (c) and (d). Cracks exist in the growth layer and run in certain directions as seen in the Figure. These cracks were generated during cooling on account of the difference of the thermal expansion coefficients between AlN and SiC.

3.2 XRD analysis of the growth layer

Crystallographic orientation of the growth layer was analyzed by performing XRD on sample B shown in Fig. 2 (c). Figure 3 shows the XRD pattern measured by θ -2 θ scan. It is found that the growth layer is oriented to c-direction of AlN as only the reflection from c-plane of AlN and SiC is detected.

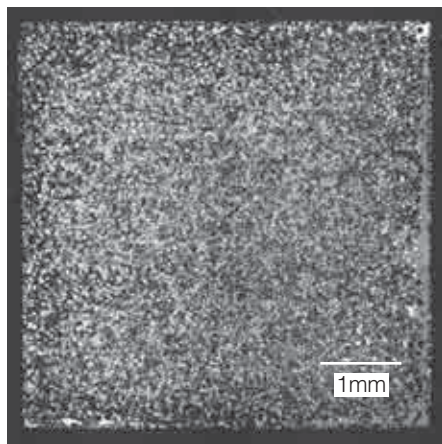
Figure 4 shows the X-ray pole figure of AlN (10 $\bar{1}$ 1) taken from the sample to investigate the symmetry of the layer. From this Figure, the 6-fold symmetric peaks are clearly identified. Thus, it is confirmed that crystallographic arrangement in the layer is highly textured.

Figure 5 shows the XRC of AlN (0002) measured on the layer. Peaks except for the main peak exist in this Figure. This is supposed to be due to the cracks generated in the AlN layer. Some divided AlN layers caused by the cracks are deviated from the original AlN layer before cracking. Therefore, it is considered that peaks from AlN layers deviated from the original plane had emerged. A full width at half maximum (FWHM) of the XRC of the AlN (0002) main peak is 650 arcsec.. From the results, it is found that the growth layer of sample B is a single crystalline AlN.

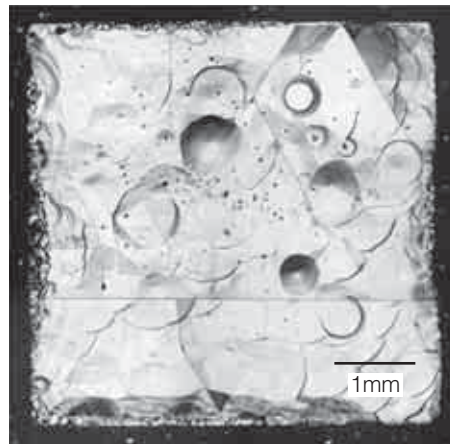
3.3 A cross-sectional observation of the growth layer

Figure 6 shows the OM image of a cross-section of the AlN growth layer. In this Figure, since the thickness of the layer is 50 μm , the growth rate of AlN single crystal in this condition is 35 $\mu\text{m h}^{-1}$.

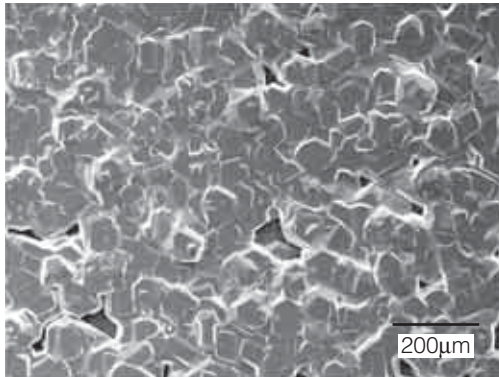
In this experiment, the reaction of AlN and SiC at the interface of AlN/SiC might happen owing to AlN crystal grown on SiC at the high temperature of 2000 $^{\circ}\text{C}$. So, the microstructure of the interface was examined by TEM observation. Figure 7 shows a lattice image of the interface. The interface is sharp and clearly separated. Consequently, the reaction rate between AlN and SiC is very low even at the high temperature of 2000 $^{\circ}\text{C}$. On the basis of this result, it was expected



(a) OM image of sample A



(c) OM image of sample B



(b) SEM image of the center part of (a)



(d) SEM image of the center part of (c)

Fig. 2. Optical microscope and SEM images showing the surface morphology of AlN grown on SiC substrates.

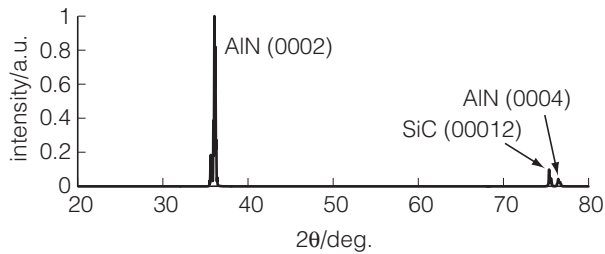


Fig. 3. X-ray diffraction pattern of sample B.

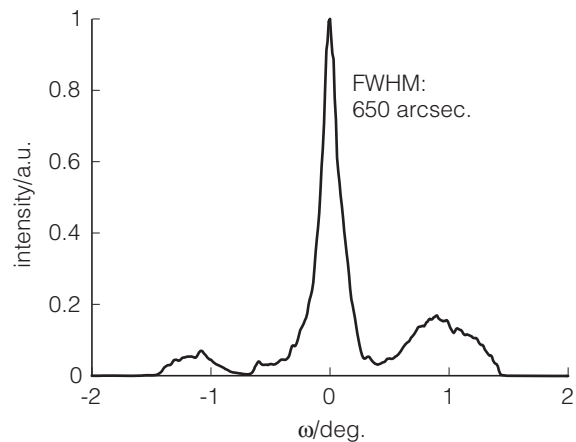


Fig. 5. X-ray rocking curve for AlN (0002) taken from sample B.

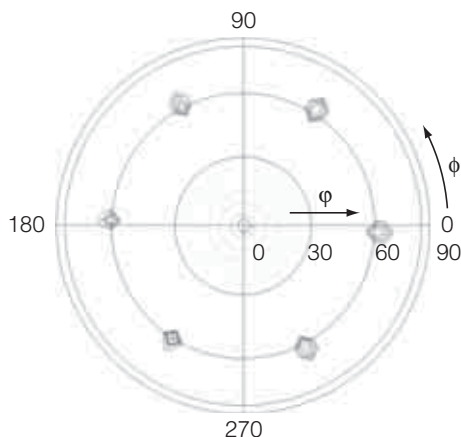


Fig. 4. X-ray pole figure for AlN (10 $\bar{1}$ 1) taken from sample B.

that thickness of AlN grown on SiC at the temperature is proportional to the time under the constant condition.

3.4 Single crystal growth of AlN on off-axis SiC (0001)

The effect of the substrates on the quality was investigated by using 6H-SiC (0001) introduced offset angle to the direction of [11 $\bar{2}$ 0]. Figure 8 shows the OM image of a surface of an AlN layer grown on the off-axis substrate (sample C) under the same condition as that

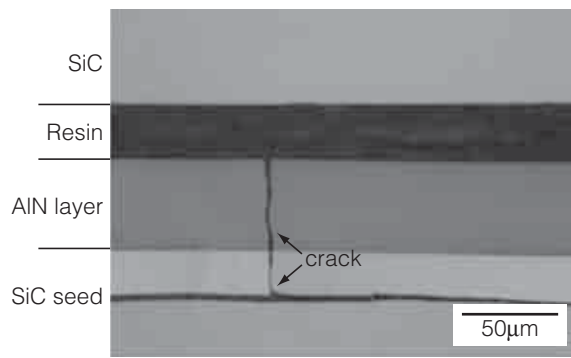


Fig. 6. Optical microscope image of a cross section of AlN growth layer on SiC shown in Fig. 2 (c) (Sample B) (SiC of the upper part was used to prevent the edge of AlN from inclining under polishing).



Fig. 7. TEM image showing a cross section of AlN/SiC interface of sample B.

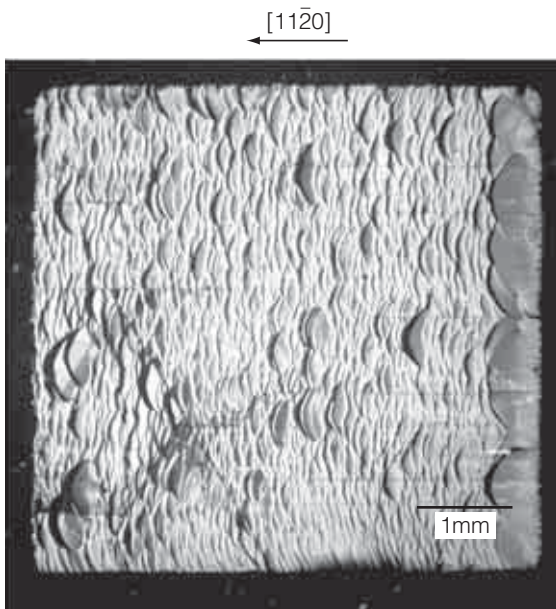


Fig. 8. Optical microscope image of a surface of AlN grown on 6H-SiC (0001) with off-axis toward $[11\bar{2}0]$ (sample C).

of sample B. This sentence is unnecessary. It need to be deleted. The growth mode is step-flow along $[11\bar{2}0]$ direction, which started from the steps introduced by the formation of offset angle. Cracks also exist in this

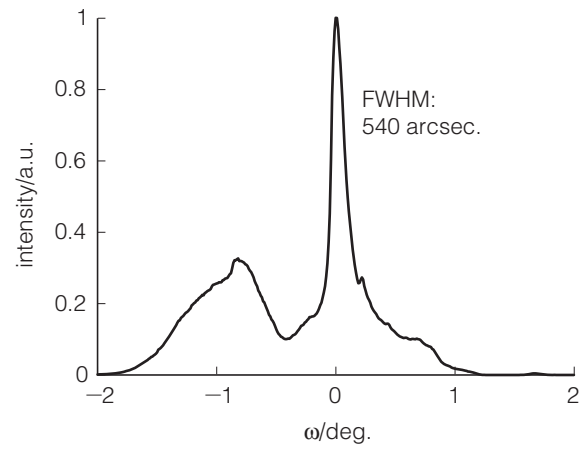


Fig. 9. X-ray rocking curve for AlN(0002) taken from sample C.

sample. From cross-sectional observation, it is found that the thickness of the layer is 50 μm , the same as that of the layer grown on the on-axis SiC substrate under the same conditions.

The XRC of AlN (0002) taken from the sample is shown in Fig. 9. FWHM is 540 arcsec. for the reflection of (0002), which is narrower than that of the crystal grown on on-axis SiC. Accordingly, it can be referred that using off-axis SiC substrates gives better crystal.

3.5 Crystal growth of thick AlN

Crystal growth of AlN for 30 h was carried out under the same condition as that of sample C with a SiC seed of 10×10 mm. Figure 10 shows the appearance and the fracture of the AlN growth layer (sample D). Amber-colored transparent AlN crystal grew on SiC and the thickness exceeded 1 mm. The thickness is in good agreement with the value estimated from the growth rate and time under this condition. Though single crystalline AlN with thickness exceeding 1 mm is obtained, cracks still exist. It is necessary to make an effort to grow thicker crystals that can endure the stress originating from the difference of the thermal expansion coefficients between AlN/SiC. The amber coloration is caused by incorporation of oxygen into AlN crystal⁵⁾. It is necessary to reduce oxygen partial pressure in the growth system by way of setting substances with a high ability of getting oxygen in the crucible.

3.6 Measurement of dislocation density by TEM

Figure 11 shows TEM images of cross-sections of the AlN growth layer represented in Fig. 10 (b). It is recognized that black dots and black lines elongating to the growth direction exist in the AlN layer in Fig. 11 (a) and (b). The dots are dislocation loops, and the lines are edge or screw dislocations. Dislocation density is calculated from division of the total number of dislocations by the TEM image areas. In the calculation, black dots on the AlN/SiC interface, which are

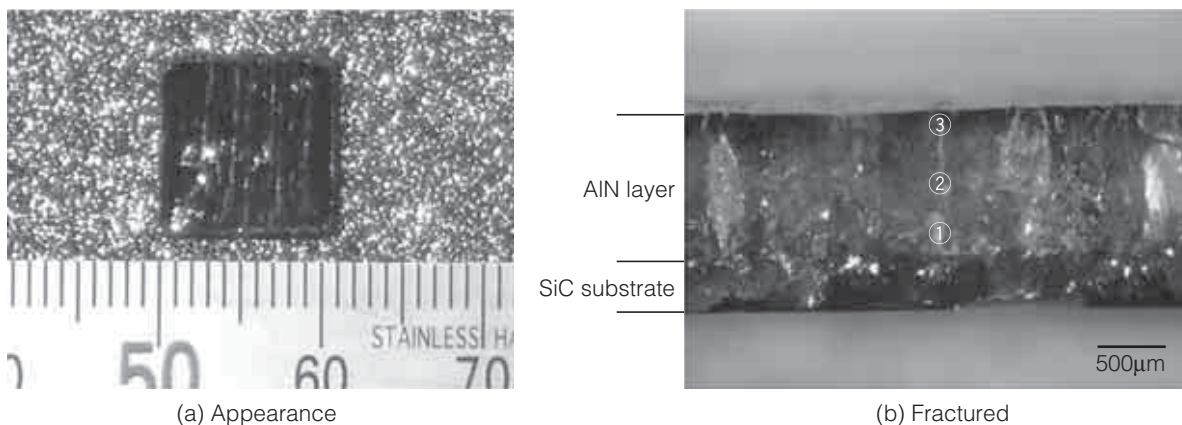


Fig. 10. Stereo microscope images of AlN grown on 6H-SiC for 30 h (sample D).

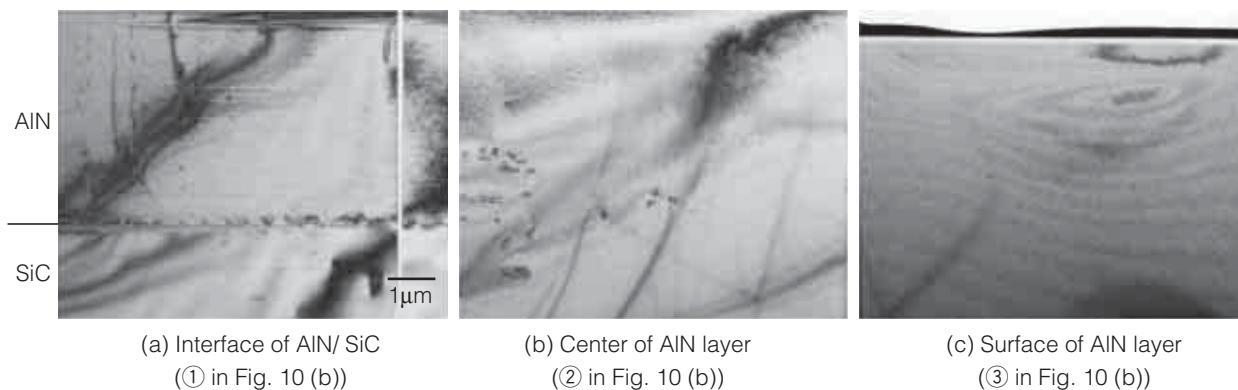


Fig. 11. Cross-sectional TEM images of sample D.

Table 2. Dislocation density calculated from cross-sectional TEM images of sample D.

Observation part	AlN/SiC interface	Center of AlN layer	Surface of AlN layer
Counted number of dislocations	33	19	0
Dislocation density/cm ⁻²	9.4×10^7	3.7×10^7	$< 2.2 \times 10^6$

misfit dislocations, were excluded. The results of the dislocation density are represented in Table 2. It is understood that the dislocation density decreases as the thickness of the AlN layer increases.

Though the chemical composition analysis was conducted to study dislocation parts and no dislocation parts by energy dispersive X-ray spectroscopy, there is no remarkable difference in the chemical composition of the both parts. In consequence, it is thought that the factor of generation of the dislocation is not incorporation of impurities, but a strain caused by a misfit between AlN/SiC. As the thickness of AlN increases, the strain becomes relaxed, and in turn the crystalline quality increases.

4. Conclusion

Single crystal growth of AlN by sublimation was

studied with the open-system crucible. As a result of this experiment, growth of a single crystalline AlN with a thickness exceeding 1 mm and high quality of the dislocation density under 10^7 cm^{-2} was successful. From the measurement of dislocation density of the crystal by TEM, it was found that crystalline quality was improved by increasing crystal thickness.

Acknowledgement

This work was financially supported by risk-taking fund for technology development from Japan Science and Technology (JST). The authors thank N. Ichinose of Waseda University who is a co-researcher of this project for his instructive guidance in the progress of this work.

References

- 1) T. P. Cho: Mater. Sci. Forum, Vol.338/342, p.1155, 2000
- 2) J. C. Rojo, L. J. Schowalter, K. Morgan, D. I. Florescu, F. H. Pollak, B. Raghoechamachar, M. Dudley: Mater. Sci. Res. Soc. Symp. Proc., Vol.680E, E2.1.1, 2001
- 3) P. B. Perry, R F. Ruz: Appl. Phys. Lett., Vol.33, p.319, 1978
- 4) Y. Taniyasu, M. Kasu and T. Makimoto: Nature, Vol.441, pp.325-328, 2006
- 5) B. M. Epelbaum, C. Seitz, A. Magerl, M. Bickermann and A. Winnacker: J. Cryst. Growth, Vol.265, pp.577-581, 2004